Microsc. Microanal. 15, 345–352, 2009
doi:10.1017/S1431927609090795

Microscopy AND Microanalysis

Zinc Mapping and Density Imaging of Rabbit Pancreas Endocrine Tissue Sections Using Nuclear Microscopy

M.D. Ynsa,[1,*] M.Q. Ren,[2] R. Rajendran,[2] J.N. Sidhapuriwala,[3] J.A. van Kan,[2] M. Bhatia,[3] and F. Watt[2]

[1]*Centro de Micro-Análisis de Materiales, Universidad Autonoma de Madrid, Campus de Cantoblanco, 28049 Madrid, Spain*
[2]*Centre for Ion Beam Applications, Department of Physics, National University of Singapore, Singapore 117542*
[3]*Department of Pharmacology, Cardiovascular Biology Research Group, Yong Loo Lin School of Medicine, National University of Singapore, 18 Medical Drive, Singapore 117597*

Abstract: Nuclear microscopy is a suite of techniques based on a focused beam of MeV protons. These techniques have the unique ability to image density and structural variations in relatively thick tissue sections, map trace elements at the cellular level to the microgram per gram (dry weight) level, and extract quantitative information on these elements. The trace elemental studies can be carried out on unstained freeze-dried tissue sections, thereby minimizing any problems of contamination or redistribution of elements during conventional staining and fixing procedures. The pancreas is a gland with different specialized cells and a complex hormonal activity where trace elements play an important role. For example, zinc has an active role in insulin production, and calcium ions participate in the stimulation and secretion process of insulin. Using nuclear microscopy with a spatial resolution of 1 μm, we have located, using zinc mapping, the islets of Langerhans in freeze-dried normal rabbit tissue sections. The islets of Langerhans contain β-cells responsible for insulin production. Subsequent quantitative analyses have indicated elevations in most elements within the islets of Langerhans, and significantly so for the concentrations of Zn [3,300 compared to 90 μg/g (dry weight)] and Ca [1,100 compared to 390 μg/g (dry weight)].

Key words: nuclear microprobe, PIXE, RBS, STIM, Zn, exocrine pancreas, endocrine pancreas

Introduction

The pancreas is composed of exocrine tissue that secretes digestive enzymes into a series of ducts for delivery into the duodenum. Scattered within the exocrine tissue are clusters of endocrine cells supported by a collagenous network containing capillaries and surrounded by a fine capsule, the islets of Langerhans, which secrete hormones into the blood stream. These islets contain several different endocrine cell types. The most abundant are insulin-producing β-cells in the core of the islets, which are surrounded by α-cells, which produce glucagon. Other less abundant endocrine cell types are δ-cells and pancreatic polypeptide (PP)-cells, which produce somatostatin and PP, respectively.

In 1934 Scott showed that insulin crystals contain Zn (Scott, 1934). Subsequent studies showed these crystals are stored within the secretory granules in the form of hexamers with two or more zinc atoms (Roth & Kirchgessner, 1981) and fluorescence imaging has shown that Zn concentrated in β-cells was related to the synthesis, storage, and secretion of insulin (Zalewski et al., 1994). While zinc is an important ion in the synthesis of insulin (Emdin et al., 1980), it is also intimately linked to the structure and action of many other enzymes involved in many different metabolic processes. For example, carboxypeptidase is a pancreatic enzyme that contains a zinc atom at the active site, and loss of the zinc in this enzyme leads to loss of activity in the pancreas (Berger & Schneeman, 1986). Since the concentrations of zinc are much higher in the islets of Langerhans than any other region (Foster et al., 1993), measurements of the Zn distribution and concentrations within the islets may provide an indication of insulin activity. It is therefore useful to develop techniques that can both image and quantitatively assess zinc and other trace elements within endocrine cells.

Nuclear microscopy is a MeV ion-based suite of techniques that has the ability to image density variations in relatively thick tissue, map trace elements at the cellular level to the microgram per gram (dry weight) level, and extract quantitative information on these elements. Nuclear microscopy is comprised of three complementary ion beam techniques that can be simultaneously applied: (a) Scanning transmission ion microscopy (STIM) is a technique in which transmitted ions (e.g., protons or helium ions—alpha particle) are detected; their energy loss in the sample is used to provide information on the structure and density variations

Received February 13, 2009; accepted May 18, 2009
*Corresponding author. E-mail: m.ynsa@uam.es

within the sample. STIM is useful for correlating the trace element data with structural features and in this study facilitates positioning of unstained sections prior to analysis. (b) Particle-induced X-ray emission (PIXE) is used for measuring the concentrations of elements such as sodium and above in the periodic table, by detecting the characteristic X-rays induced by MeV protons. (c) Rutherford backscattering spectrometry (RBS) provides information on matrix composition and incident charge, and is used in conjunction with PIXE to quantify the trace element concentration results (Watt & Grime, 1995).

Although nuclear microscopy techniques cannot yet be applied to living cells, its unique capability of mapping and measuring quantitative trace element concentrations at the cellular level make it a powerful tool for biomedical studies. Previous nuclear microprobe work on measuring trace elements in the pancreas has been limited to mice pancreas studies, using low resolution PIXE in conjunction with a nuclear microprobe (Lindh et al., 1985, 1991; Juntti-Berggren et al., 1987, 1991). Starvation was used as a model for altered glucose recognition by the β-cells and altered elemental composition (Al, Cu, Mg, Rb, Ca, and Zn) of endocrine pancreas was found to be dependent on the time of starvation (Juntti-Berggren et al., 1991; Lindh et al., 1991). The K/Na ratio was studied in genetically diabetic Chinese hamsters and normal controls (Lindh et al., 1985; Juntti-Berggren et al., 1987). The fact that β-cells from diabetic Chinese hamsters maintain physiological intracellular levels of Na and K indicates the existence of a well-functioning Na^+/K pump. The role that Ca^{2+} has in stimulating the secretion of insulin and the secretion itself has also been studied analyzing cultured cells with nuclear microprobe techniques (Pålsgård et al., 1994, 1995; Pålsgård & Grime, 1996). In these studies, strontium was used as a tracer to discriminate between endogenous calcium and Ca^{2+} entering as a result of stimulation. Different Zn isotopes have also been imaged in the islets of Langerhans using secondary ion mass spectrometer (Okabe et al., 2003) and fluorescence techniques (Zalewski et al., 1994), although these techniques are not quantitative.

In this article we describe the methodology and protocol for carrying out nuclear microscopy of the exocrine pancreas regions of normal rabbits and present the results of zinc imaging, quantitative trace elemental analysis using PIXE and RBS, and density mapping using STIM.

Material and Methods

Sampling

Three normal male New Zealand white rabbits of the same age, weighing approximately 2.5 kg were used for this study. The animals (which were normal controls for another study on trace elements in atherosclerosis) were killed by i/v injection of sodium pentobarbitone (0.8 mg/kg) and two pancreas sections just below the spleen were removed. Residual blood was removed from the tissue by flushing with deionized water, and the blocks of tissue were then flash frozen in liquid nitrogen. The tissue was stored at -80°C and transported on dry ice where necessary. Special care was taken to prevent thawing and refreezing and subsequent ice crystal damage. Serial sections of thicknesses 10 μm were cut using a Leica CM3050S cryostat set at -17°C with the knife at -22°C. Sections were picked up on gelatin-coated glass slides for hematoxylin and eosin staining to identify regions of interest. Adjacent unstained sections were picked up on freshly made 0.5 μm pioloform film mounted on nuclear microscopy target holders for STIM, RBS, and PIXE analysis.

Experimental

The pancreas sections were analyzed using the nuclear microscope facility at the Centre for Ion Beam Applications (CIBA), National University of Singapore (Watt et al., 1994), where PIXE, RBS, and STIM techniques can be used simultaneously. A beam of 2.1 MeV protons focused to a diameter of about 1 μm were used for this work. The incident proton beam was at 45° to the sample surface and the beam current was in the range of 100–300 pA. Transmitted particles (STIM) were detected using an ion-implanted silicon charged particle detector placed off beam axis (at 20° to the beam). A lithium-drifted silicon detector at 90° to the beam, with a 300 μm Perspex® filter with a 1-mm-diameter central hole was used to detect X-rays (PIXE). For RBS analysis, backscattered protons were detected using a silicon particle detector at a scattering angle of 160° to the beam.

High-resolution STIM was also carried out using a second beam line facility at CIBA. Here the high-resolution proton beam writer line was used, where the target chamber was modified slightly to incorporate a miniature STIM target assembly. As described in Ren et al. (2007), the target assembly was constructed utilizing a Hamamatsu pin diode S1223-01 (3.06×3.06 mm^2 chip), which was mounted directly behind the pioloform film on which the pancreas section was placed. A 1.5 MeV alpha particle beam, which has an order of magnitude increase in stopping power compared with a proton beam, was focused with a size of 45×65 nm^2 and scanned across a suitable area of the pancreas.

For the extraction of quantitative elemental concentrations, PIXE and RBS spectra were obtained from regions of interest after identification of structures using the elemental and STIM maps. Analysis of RBS spectra allowed both quantification of lights elements such as C, N, and O, thereby characterizing the tissue matrix, as well as measurement of areal density. The RBS data were analyzed by fitting the RBS spectra using SIMNRA (Mayer, 1997) software. This technique was also used for integrated charge correction, thus enabling quantitative data to be extracted from PIXE spectra by GUPIX (Maxwell et al., 1989). Means and standard devia-

tions were used as the descriptive statistics. To determine if there were significant differences for the elemental concentrations between and among groups, the parametric Student t-test and nonparametric (NP) approaches such as the Kolmogorov-Smirnov test, the Mann-Whitney U-test, and the Wald-Wolfowitz test (Woolson, 1987) were used. Differences were considered significant when a confidence interval of 95% was exceeded ($p < 0.05$). For STIM imaging, a median transmitted energy was calculated for each image pixel using the OMDAQ software package to provide suitable density contrast and to reduce the amount of noise in the image.

Results

The normal protocol for identifying structures prior to nuclear microscopy imaging is to first carry out a proton STIM image of an unstained section and compare this to the optical image of a serial stained section. A visual comparison usually reveals areas of interest that can then be located in the unstained tissue by subsequent high-magnification STIM imaging. For this work, proton STIM imaging was not used to determine the position of the islets of Langerhans because the density and shape of this group of cells were not sufficiently different from surrounding exocrine cells to allow a positive identification. Instead, it proved more reliable for identification purposes to use zinc mapping. Figure 1 shows a stained section of tissue (Fig. 1a) and a corresponding proton STIM image of an unstained serial section (Fig. 1b). The islets of Langerhans observed in the stained section (red circles) cannot be identified clearly by proton STIM imaging at this magnification. However, simultaneous zinc mapping (Fig. 1c) indicates the position of the islets of Langerhans. The lower magnification image (4 mm × 4 mm) shown in Figure 2 confirms that zinc mapping can be used for relatively large area tissue sections to locate the islets of Langerhans.

An area containing an islet of Langerhans was subsequently imaged at higher resolution (120 μm × 120 μm), and the proton STIM image and the zinc map are shown in Figure 3. Also included is a sulfur and iron image of the same region. These results indicated a clear inverse correlation between the iron and zinc distributions, which was also reproduced in other scans.

After the identification of islets of Langerhans, the elemental concentrations taken from the endocrine and exocrine pancreas were determined. Table 1 shows the average P, S, Cl, K, Ca, Fe, and Zn concentrations and the standard deviation. Although all the values appear higher in endocrine tissue than exocrine, the t-test and NP tests only showed significant differences between endocrine and exocrine pancreas for S, Ca, and Zn. Averaging of the results from all three rabbits, elemental analyses from 11 regions of the endocrine pancreas showed higher concentration variability than from the exocrine tissue determined in 7 regions. Generally, the concentration variability of elemental concentration in biological tissues is high. Although we have only analyzed normal pancreas, we cannot assume that the variability of elements and the elemental concentrations are the same in all cells.

Table 1. Average Concentration and Standard Deviation in μg/g (dry weight) of Endocrine and Exocrine Pancreas of Normal Rabbits.

	Endocrine Pancreas $\bar{x} \pm$ std (μg/g)	Exocrine Pancreas $\bar{x} \pm$ std (μg/g)
P	18,000 ± 3,000	14,000 ± 5,000
S	6,900 ± 800	4,600 ± 1,600
Cl	6,300 ± 1,800	4,300 ± 1,600
K	20,000 ± 8,000	14,000 ± 5,000
Ca	1,100 ± 300	390 ± 140
Fe	170 ± 90	86 ± 19
Zn	3,300 ± 1,200	90 ± 19

For low demagnification, proton STIM imaging did not allow for positive identification of the islets of Langerhans in unstained sections. We therefore investigated the structure of individual cells within the islets of Langerhans using STIM operating with a 50 nm alpha particle beam. Figure 4a shows an alpha STIM image of a 180 × 180 μm^2 region of tissue containing an islet of Langerhans. Consecutive smaller scans of 60, 20, and 10 μm^2 are shown in Figure 4b–d and indicate subcellular structure of high contrast.

Discussion

Elemental Study

Zinc is an essential cofactor for the gene expression, synthesis, conformation, storage, and secretion of insulin (Chausmer, 1998). Decreased plasma zinc impairs the ability of islet cells to produce and secrete insulin and deficiency results in rapid insulin degradation (Quarterman et al., 1966; Huber & Gershoff, 1973; Reid, 1981; Prasad, 1985). Insulin is produced by the beta cell of the pancreatic islets as a single chain peptide that is bent around itself and linked by two interchain disulfide bonds. This proinsulin is cleaved by the removal of an intracellular chain fragment known as the "C-peptide" to form two peptide chain (alpha and beta) molecules of 51 amino acids crosslinked to each other by interchain disulfide bonds. This is the insulin monomer. In the presence of zinc within the cell, insulin monomers assemble to a dimeric form for storage and secretion as the zinc crystal. It has been shown that high concentrations of glucose and other secretagogues decrease the islet cell labile Zn, and video fluorescence analysis

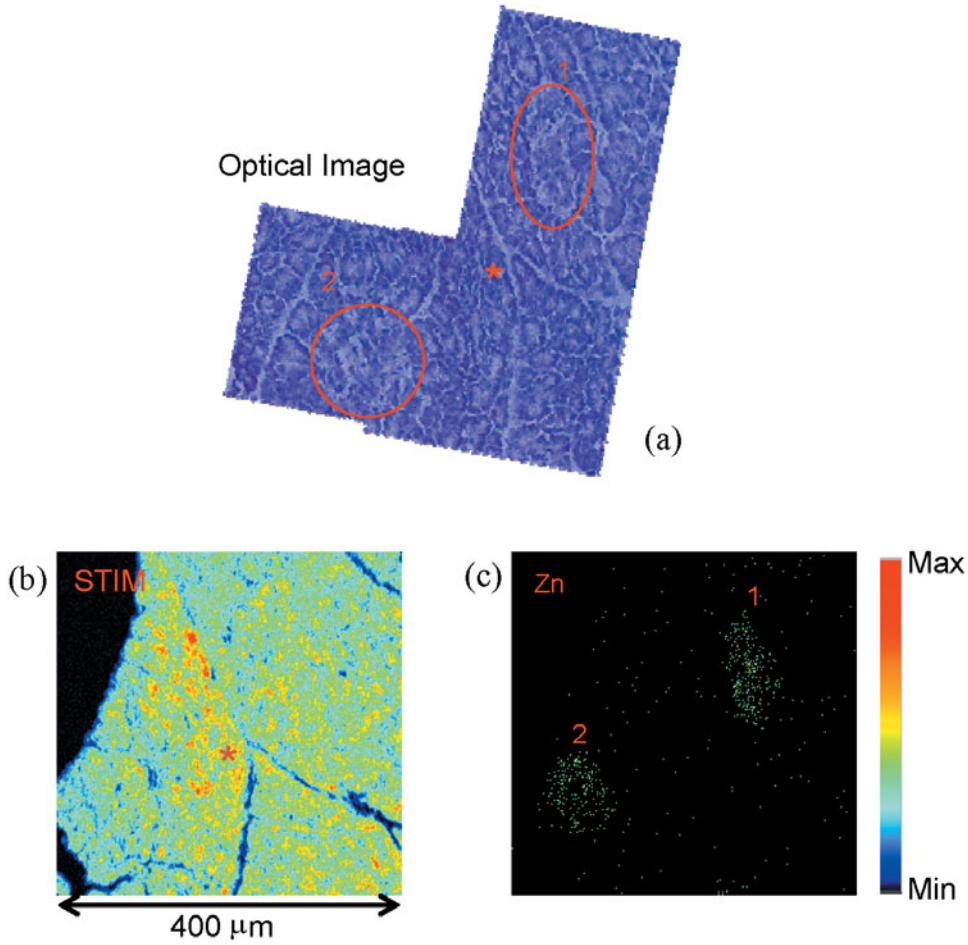

Figure 1. (**a**) Optical image of an H&E serial stained section of normal rabbit pancreas, (**b**) proton STIM map, and (**c**) Zn map. The low density tissue intersection near the center of the STIM image (marked with an asterisk) can be correlated with the optical image of the stained section. The islets of Langerhans, which can be identified in the optical image (red circle) of the stained section, are not easily defined in the STIM image. The zinc map, however, shows that the positions of the islets of Langerhans can be identified through their higher zinc concentrations.

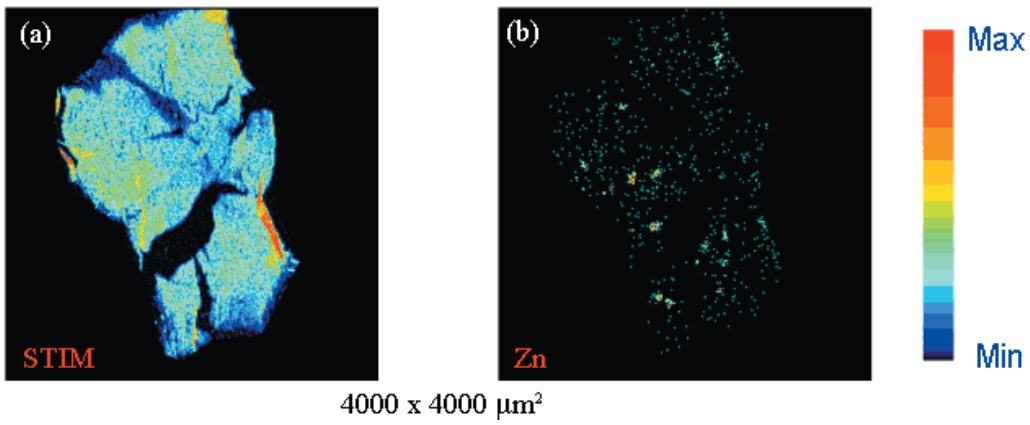

Figure 2. (**a**) Proton STIM and (**b**) Zn maps of a normal rabbit pancreas section. Regions with high Zn concentration can be observed in Zn map. These regions correspond to the islets of Langerhans by comparison with serial stained sections (not shown).

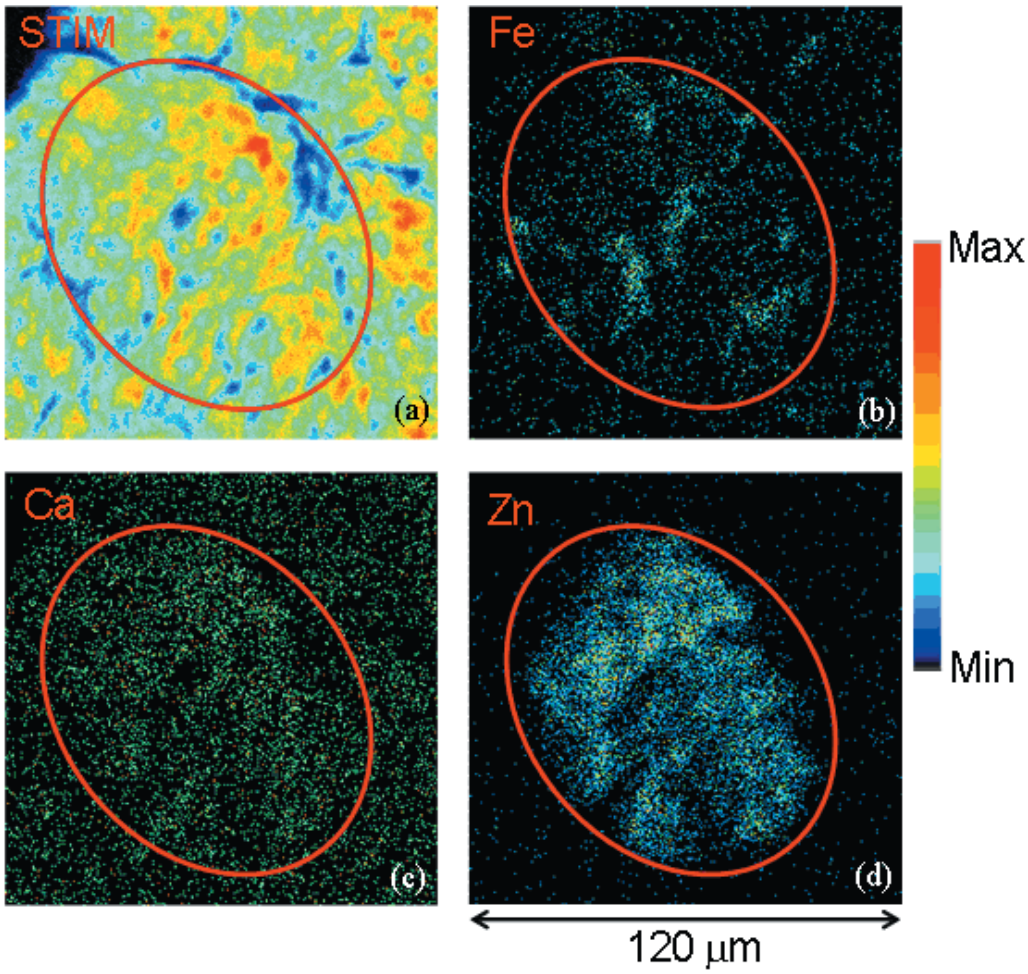

Figure 3. (**a**) Density (proton STIM), (**b**) Fe, (**c**) Ca, and (**d**) Zn maps of an islet of Langerhans. An anticorrelation between Fe and Zn and a correlation between Ca and Zn were shown. The Ca image contains relatively few counts because we utilized the reduced yield Ca-K_β X-ray peak (the Ca-K_α X-ray peak has an interfering K-K_β peak).

showed Zn concentrated in the islet cells was related to the synthesis, storage, and secretion of insulin (Zalewski et al., 1994). Zinc fluxes and zinc transporter genes have been shown to play a key role in chronic diseases, such as diabetes (Devirgiliis et al., 2007; Murgia et al., 2008)

Potassium and calcium in the endocrine pancreas are necessary for optimal insulin secretion. The increase of glucose levels in blood provokes the closure of ATP-dependent potassium channels that produces an increase of the cytosolic Ca^{2+} concentration $[Ca^{2+}]_{cyt}$ due to the depolarization of the plasma membrane. The $[Ca^{2+}]_{cyt}$ rise is essential for the initiation of insulin secretion, and all the β-cells within the same islet of Langerhans have a synchronous and homogeneous $[Ca^{2+}]_{cyt}$ oscillatory pattern. Insulin secretion therefore is pulsatile, coinciding with the peaks of $[Ca^{2+}]_{cyt}$ (Valdeolmillos et al., 1992). However, the endocrine Ca concentration detected in these rabbit pancreas samples is too high to be only associated with this mechanism. Calmodulin is the primary cellular receptor for calcium, and the interaction between calcium and calmodulin is analogous to the binding of a steroid hormone to its cognate receptor. Calcium plays a fundamental role in cell signaling. Here, increased calcium concentration in endocrine pancreas might have been utilized in Ca^{2+}/calmodulin-dependent protein kinase pathway for insulin secretion (Ashcroft et al., 1994).

Sulfur is found in two amino acids and participates as an enzyme cofactor. Despite the increased knowledge on the role of amino acids, their exact role in endocrine function still remains unanswered. Several studies demonstrate that intake of sulfur-containing amino acid has a beneficial effect in overcoming insulin resistance (Maturo & Kulakowski, 1988; Anitha Nandhini et al., 2005; Blouet et al., 2007). This fact could be due to an active function of these amino acids in the insulin production process, which could explain the elevated concentration of S in endocrine pancreas.

The Fe maps of the islets of Langerhans as shown in Figure 3 show a nonhomogenous distribution that is nega-

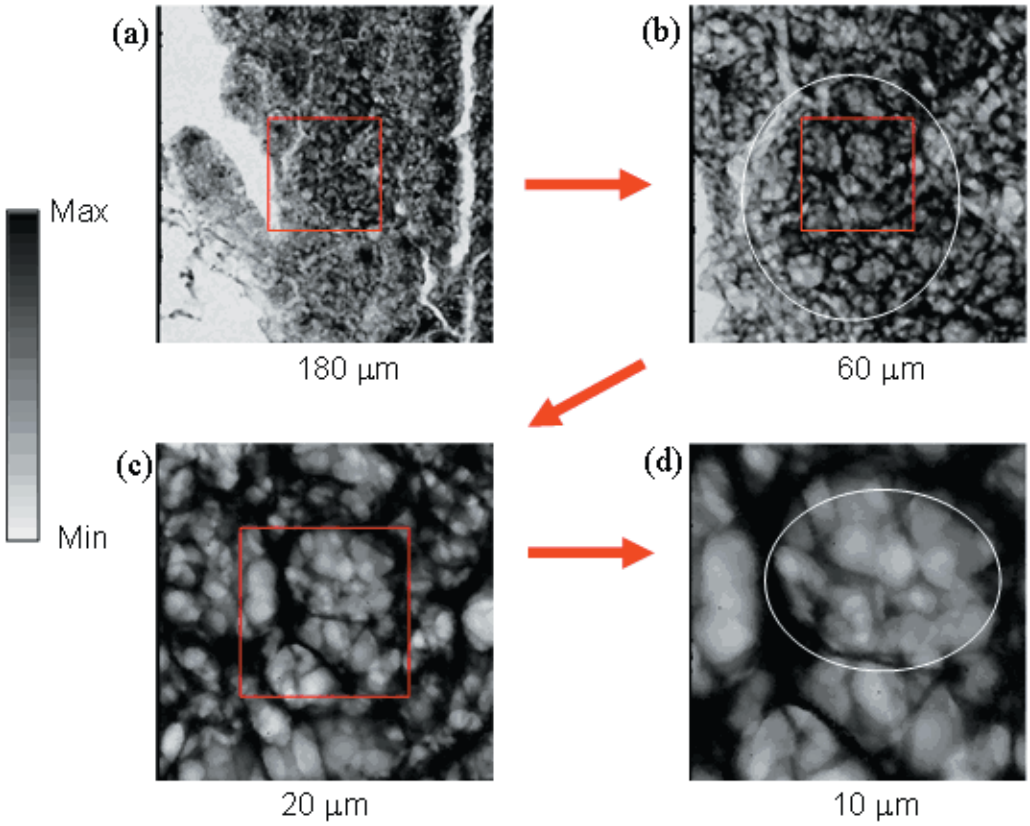

Figure 4. Increasing high-resolution alpha STIM images obtained using a sub-100 μm beam (45 $\times$ 65 nm^2) of unstained pancreas 10 μm tissue sections. Scan sizes are (**a**) 180 μm^2, (**b**) 60 μm^2, (**c**) 20 μm^2, and (**d**) 10 μm^2. The 60 μm^2 scan indicates an islet of Langerhans (white circle), and the 10 μm^2 scan indicates a beta cell (white circle) within the islet showing neurosecretory vesicles.

tively correlated with Zn. The capillaries with residual blood in the islets of Langerhans could explain the elevated levels of iron in the endocrine tissue, and also the anticorrelation between the Fe and Zn distribution.

Although the t-test did not show significant differences between Cl concentration in exocrine tissue and islets of Langerhans, the slightly elevated concentration found in the endocrine tissue suggests that this element may have a role in the islets of Langerhans. Previous studies suggested that anions, e.g., phosphate, bicarbonate, and chloride, may also play an important role in the regulation of insulin release, indicating a possible function for chloride in the regulation of the membrane potential in the pancreatic β-cells (Lindstrom et al., 1988).

Density Study

The size of the structures and the type of the polyhedric inclusions observed in Figure 4 are typical of islets of Langerhans. From Figure 4a we can identify an islet of Langerhans separated from the exocrine tissue by a thin pod of less dense tissue. These regions could be connective tissue that normally surrounds the islets of Langerhans. β-cells are smaller than the cells outside islets of Langerhans, thus the dimensions of the identified central structures lead us to conclude that this organization is a β-cell. The lower density inclusion is likely to be vesicles that are found in β-cells. The insulin grains are normally inside the neurosecretory vesicles, which have dimensions approximately 300 nm, consistent with structures in our high-resolution STIM images. The vesicles that produce insulin normally have a central electron-dense core, consisting of insulin in the form of rhomboidal or polyhedral crystalline structures surrounded by an electron-lucent halo and bounded by a narrow membrane. Our images suggest that the β-cell vesicles in this particular region have been voided, possibly indicating a recent discharge of insulin.

Conclusions

Nuclear microscopy, consisting of a suite of techniques encompassing PIXE, STIM, and RBS, has the ability to image density variations in relatively thick tissue, map trace elements at the cellular level, and extract quantitative infor-

mation on these elements to the parts per million level. The role of nuclear microscopy is ideally suited to mapping important trace elements such as Zn, Ca, Fe, and Cu in tissue and cells, and extracting quantitative data. These analyses can be carried out in unstained freeze-dried tissue sections, thereby minimizing any problems of contamination or redistribution of elements during sample preparation.

For this animal model, we have shown that islets of Langerhans can be identified in freeze-dried and unstained tissue sections using zinc mapping. Proton STIM, which is normally used to identify structures prior to quantitative analysis, however, is not as effective for identification due to minimal density and structural variations between the endocrine and exocrine regions. Once identified, elemental analysis can be carried out, and the difference in elemental concentrations between the islets of Langerhans and the surrounding tissue can be assessed. However, we cannot assume that this method is ideal for other animal models where Zn concentrations may be lower.

These analyses have indicated elevations in most elements within the islets of Langerhans, and significantly so for the concentrations of Zn [3,300 compared to 90 μg/g (dry weight)], Ca [1,100 compared to 390 μg/g (dry weight)]. The high levels of Zn, Ca, K, Cl, and S concentrations detected in the endocrine pancreas confirm the high biological activity of this region because these elements are involved in numerous biological processes such as intracellular signal transduction and synthesis, storage, and release of insulin.

It is only recently that sub-100 nm STIM has been available, and this new technique has been used to image β-cells within the islets of Langerhans. We have demonstrated the potential of alpha STIM in identifying both cells and strategic vesicles within these cells. The state of the art spatial resolution for quantitative elemental analysis at the microgram per gram (dry weight) level is around 300 nm, and the state of the art resolutions for STIM is currently 50 nm. Although STIM is still some way short of the excellent resolutions of scanning electron microscopy and transmission electron microscopy, which can be down to the nanometer level and below, we are hoping to improve this in the near future. The real potential of structural imaging using high energy ions, however, is that it can be used on whole cells and relatively thick tissue. Unlike electrons, fast ions maintain resolution through thicker samples, and as such nuclear microscopy has the potential to provide high-resolution three-dimensional information.

Acknowledgments

The research of the first author was supported by the program Jose Castillejo of the Spanish Ministerio de Educación y Ciencia. We also wish to thank Teresa Pinheiro for discussions on the interpretation of the pancreatic beta cell structure.

References

Anitha Nandhini, A.T., Thirunavukkarasu, V. & Anuradha, C.V. (2005). Taurine modifies insulin signalling enzymes in the fructose-fed insulin resistant rats. *Diab Metabolism* **31**, 337–344.

Ashcroft, F.M., Proks, P., Smith, P.A., Ammälä, C., Bokvist, K. & Rorsman, P. (1994). Stimulus-secretion coupling in pancreatic beta cells. *J Cell Biochem* **55**, 54–65.

Berger, J. & Schneeman, B.O. (1986). Stimulation of bile-pancreatic zinc, protein and carboxypeptidase secretion in response to various proteins in the rat. *J Nutr* **116**, 265–272.

Blouet, C., Mariotti, F., Azzout-Marniche, D., Mathé, V., Mikogami, T., Tomé, D. & Huneau, J.F. (2007). Dietary cysteine alleviates sucrose-induced oxidative stress and insulin resistance. *Free Rad Biol Med* **42**, 1089–1097.

Chausmer, A.B. (1998). Zinc, insulin and diabetes. *J Am Coll Nutr* **17**, 109–115.

Devirgiliis, C., Zalewski, P.D., Perozzi, G. & Murgia, C. (2007). Zinc fluxes and zinc transporter genes in chronic diseases. *Mutat Res* **622**, 84–93.

Emdin, S.O., Dodson, G.G., Cutfield, J.M. & Cutfield, S.M. (1980). Role of zinc in insulin biosynthesis. Some possible zinc-insulin interactions in the pancreatic B-cell. *Diabetologia* **19**, 174–182.

Foster, M.C., Leapman, R.D., Li, M.X. & Atwater, I. (1993). Elemental composition of secretory granules in pancreatic islets of Langerhans. *Biophys J* **64**, 525–532.

Huber, A.M. & Gershoff, S.N. (1973). Effect of zinc deficiency in rats on insulin release from the pancreas. *J Nutr* **103**, 1739–1744.

Juntti-Berggren, L., Lindh, U. & Berggren, P.O. (1991). Starvation is associated with changes in the elemental composition of the pancreatic beta-cell. *Biosci Rep* **11**, 73–84.

Juntti-Berggren, L., Lindh, U., Berggren, P.O. & Frankel, B.J. (1987). Proton microprobe analysis of 15 elements in pancreatic B cells and exocrine pancreas in diabetic Chinese hamsters. *Biosci Rep* **7**, 33–41.

Lindh, U., Juntti-Berggren, L., Berggren, P.O. & Hellman, B. (1985). Proton microprobe analysis of pancreatic beta-cells. *Biomed Biochim Acta* **44**, 55–61.

Lindh, U., Sunde, T., Juntti-Berggren, L., Berggren, P.O. & Pålsgård, E. (1991). Nuclear microscopy and the application to diabetes research. *Nucl Instrum Methods B* **56/57**, 1279–1283.

Lindstrom, P., Norlund, L., Sandstrom, P.E. & Sehlin, J. (1988). Evidence for co-transport of sodium, potassium and chloride in mouse pancreatic islets. *J Physiol* **400**, 223–236.

Maturo, J. & Kulakowski, E.C. (1988). Taurine binding to the purified insulin receptor. *Biochem Pharmacol* **37**, 3755–3760.

Maxwell, J.A., Campbell, J.L. & Teesdale, W.J. (1989). The Guelph PIXE software package. *Nucl Instrum Methods B* **43**, 218–230.

Mayer, M. (1997). SIMNRA User's Guide. Technical Report IPP 9/113, Max-Planck-Institut für Plasmaphysik, Garching, Germany.

Murgia, C., Devirgiliis, C., Mancini, E., Donadel, G., Zalewski, P. & Perozzi, G. (2008). Diabetes-linked zinc transporter ZnT8 is a homodimeric protein expressed by distinct rodent endocrine cell types in the pancreas and other glands. *Nutr Metab Cardiovasc Dis* **19**, 431–439.

Okabe, M., Yoshida, T., Yoshii, R., Sawataisi, M. & Takaya, K. (2003). Zinc detection in the islet of Langerhans by SIMS. *Appl Surf Sci* **203–204**, 714–717.

Pålsgård, E. & Grime, G.W. (1996). Direct measurement of elemental distributions in insulin-producing cells using nuclear microscopy. *Cell Mol Biol* **42**, 49–57.

Pålsgård, E., Lindh, U., Juntti-Berggren, L., Berggren, P.O., Roomans, G.M. & Grime, G.W. (1994). Proton-induced and electron-induced X-ray microanalysis of insulin-secreting cells. *Scanning Microsc Suppl* **8**, 325–332.

Pålsgård, E., Roomans, G. & Lindh, U. (1995). Ion dynamics in cells—Preparation for studies of intracellular processes. *Nucl Instrum Methods B* **104**, 324–327.

Prasad, A.S. (1985). Clinical, endocrinologic, and biochemical effects of zinc deficiency. *Spec Top Endocrinol Metab* **7**, 45–76.

Quarterman, J., Mills, C.F. & Humphries, W.R. (1966). The reduced secretion of, and sensitivity to insulin in zinc-deficient rats. *Biochem Biophys Res Commun* **25**, 354–358.

Reid, G.M. (1981). The pharmacological role of zinc: Evidence from clinical studies on animals. *Med Hypotheses* **7**, 207–215.

Ren, M.Q., van Kan, J.A., Bettiol, A.A., Daina, L., Gek, C.Y., Huat, B.B., Whitlow, H.J., Osipowicz, T. & Watt, F. (2007). Nano-imaging of single cells using STIM. *Nucl Instrum Methods B* **260**, 124–129.

Roth, H.P. & Kirchgessner, M. (1981). Zinc and insulin metabolism. *Biol Trace Elem Res* **3**, 13–32.

Scott, D.A. (1934). Crystalline insulin. *Biochem J* **28**, 1592–1602.

Valdeolmillos, M., Nadal, A., Contreras, D. & Soria, B. (1992). The relationship between glucose-induced K+ATP channel closure and the rise in $[Ca^{2+}]_i$ in single mouse pancreatic β-cells. *J Physiol* **455**, 173–186.

Watt, F. & Grime, G.W. (1995). The high-energy ion microprobe. In *Particle-Induced X-Ray Emission Spectrometry (PIXE)*, Johansson, S.A.E., Campbell, J.L. & MalmQvist, K.G. (Eds.), pp. 101–165, Chemical Analysis Series, Vol. 133. New York: John Wiley & Sons, Inc.

Watt, F., Orlic, I., Loh, K.K., Sow, C.H., Thong, P., Liew, S.C., Osipowicz, T., Choo, T.F. & Tang, S.M. (1994). The National University of Singapore nuclear microscope facility. *Nucl Instrum Methods B* **85**, 708–715.

Woolson, R.F. (1987). *Statistical Methods for the Analysis of Biomedical Data*. New York: John Wiley & Sons.

Zalewski, P., Millard, S., Forbes, I., Kapaniris, O., Slavotinek, S., Betts, W., Ward, A., Lincoln, S. & Mahadevan, I. (1994). Video image analysis of labile Zn in viable pancreatic islet cells using specific fluorescent probe for Zn. *J Histochem Cytochem* **42**, 877–884.